

Evidence Against Direct Connections to PPRF EBNs From SC in the Monkey

E. L. KELLER, R. M. McPEEK, AND T. SALZ

Smith-Kettlewell Eye Research Institute, San Francisco, California 94115

Received 18 January 2000; accepted in final form 24 May 2000

Keller, E. L., R. M. McPeek, and T. Salz. Evidence against direct connections to PPRF EBNs from SC in the monkey. *J Neurophysiol* 84: 1303–1313, 2000. Direct projections from the superior colliculus (SC) to the paramedian pontine reticular formation (PPRF) have been demonstrated anatomically. The PPRF contains cells called excitatory burst neurons (EBNs) that execute the final premotoneuronal processing for saccadic eye movements, as well as other burst cells called long-lead burst neurons (LLBNs). Previous electrophysiological tests in monkey have failed to find evidence for monosynaptic connections from the SC to EBNs, but have shown that direct projections to LLBNs exist. The validity of these results has been questioned because EBNs are known to be inhibited during periods of fixation by cells called omnipause neurons (OPNs). In later experiments in cat, the stimulus in the SC was triggered during saccades (when OPNs are off) and direct connections to EBNs were found. The present experiments were conducted to determine whether direct connections from the SC to EBNs could be demonstrated in monkey. LLBNs located near EBNs were also recorded. Single-pulse stimuli were delivered at sites in the SC at current levels well above those required to evoke saccades with pulse train stimuli. The stimuli were triggered shortly after the onset of ipsilateral or contralateral saccades and also slightly after the end of saccades. A sample of 21 EBNs was recorded and none were activated by postsaccadic stimulation or during contralateral saccades. The high spontaneous discharge rates of EBNs during ipsilateral saccades made activation of these cells more difficult to detect; however, when the results were quantified by peristimulus time histograms aligned on stimulus onset, only 1/21 EBNs showed evidence of activation in the monosynaptic range of latencies (<1.6 ms), 13 EBNs were activated at di- or polysynaptic latencies, and 7 were not activated. In contrast, 15/21 LLBNs were activated with latencies in the monosynaptic range. Further evidence supporting the absence of direct connections to EBNs was obtained by realigning the peristimulus time histograms for a subset of EBNs with similar firing rates on the time of occurrence of the last spike before stimulus onset. A subset of EBNs was also studied during drowsy ipsilaterally directed eye drifts, during which these cells were firing at low spontaneous rates and OPNs were off. No evidence for direct connections to EBNs was found in this behavioral state. The variance in results obtained for cat and monkey may be due to a species difference that reflects the more complex signal processing required in the monkey's saccadic system.

INTRODUCTION

The role of a group of premotor neurons called excitatory burst neurons (EBNs), which are found in the paramedian pontine reticular formation (PPRF), in the generation of sac-

cadic eye movements has been well studied (for reviews see Fuchs et al. 1985; Keller 1991; Moschovakis et al. 1996). They are known to project directly to abducens motoneurons and indirectly to medial rectus motoneurons (through abducens internuclear neurons) and are believed to provide the main excitatory drive to both types of motoneurons during horizontal saccades. Pools of EBNs are located in the reticular formation just rostral to the abducens nucleus, and they discharge an intense burst of spikes during ipsilaterally directed saccades. The duration of this burst closely approximates the duration of the saccade, and the frequency of the burst is monotonically related to saccadic velocity. This group of cells plays a key role in all current models of saccade generation.

In spite of the wealth of knowledge that has been obtained about this distinct group of cells and their vertical-direction counterparts that are located in the interstitial nucleus of the medial longitudinal fasciculus (riMLF), the nature of the connections to EBNs from upper level sensorimotor structures such as the superior colliculus (SC) and the cortical frontal eye fields (FEF) remains unclear. The existence of direct connections to the region of the EBNs from both the SC and the FEF has been shown by anatomic means (Harting 1977; Leichnetz et al. 1984; Olivier et al. 1993; Stanton et al. 1988). Nevertheless, when Raybourn and Keller (1977) stimulated the deeper layers of the SC in the alert monkey, they were unable to activate EBNs with single-pulse stimuli, although they did produce activation of EBNs following triple-pulse stimuli with resultant latencies in the poly-synaptic range. Segraves (1992) reported similar results for stimuli delivered to the FEF. In the study of Raybourn and Keller, another group of neurons called long lead burst neurons (LLBNs), which were also found in the PPRF in close proximity to EBNs, was readily activated from the SC, many in the range of latencies suggesting monosynaptic connections. The LLBNs are a more heterogeneous group of PPRF neurons that show a prelude of discharge long before saccade onset as well as a burst of activity during saccades (Fuchs et al. 1985; Hepp and Henn 1983; Keller 1991). The characteristics of the saccade-linked burst in LLBNs are not as clearly related to saccadic parameters such as duration and velocity as are those of EBNs (Fuchs et al. 1985; Keller 1991). Raybourn and Keller (1977) suggested that at least some of the LLBNs form an earlier stage of neural signal processing possibly involved in the conversion of place-coded information

Address for reprint requests: E. L. Keller, Smith-Kettlewell Eye Research Institute, 2318 Fillmore St., San Francisco, CA 94115 (E-mail: elk@ski.org).

The costs of publication of this article were defrayed in part by the payment of page charges. The article must therefore be hereby marked "advertisement" in accordance with 18 U.S.C. Section 1734 solely to indicate this fact.

from SC and FEF to the temporal code used by EBNs, which in turn project to motoneurons.

Raybourn and Keller (1977) also pointed out a possible procedural shortcoming in their experiments. They had delivered their stimuli in the SC [as had Segraves (1992) in the FEF] with the monkey fixating a visual target. During this behavioral state it is known that omnipause neurons (OPNs), a group of cells located near the midline of the brain stem and that directly inhibit EBNs (Strassman et al. 1987), are discharging at high rates. The tonic inhibition provided to EBNs by OPNs may have prevented the detection of monosynaptic connections with the extra-cellular recording techniques that were used in their study.

Chimoto et al. (1996) recently tested this suggestion. They recorded EBNs and inhibitory burst neurons (IBNs) in the cat while delivering single-pulse stimuli to the deeper layers of the SC, but they delivered these stimuli during saccades when OPNs are turned off. They reported that strong monosynaptic connections could be demonstrated when the stimulation was delivered during saccadic movements. In the present study, we used similar techniques to Chimoto et al. (1996), but now in the monkey to determine whether a similar pattern of direct connections could be demonstrated in this species. This is an important question, because the output neurons in the deeper layers of the SC, as well as those in the FEF, are organized with spatial coding. At the same time it is clear that EBNs are temporally coded. There have been attempts to explain the transformation of spatial coding to temporal coding (Moschovakis et al. 1998), but if this complex signal processing step occurs at the level of a direct projection to EBNs, the range of mechanisms that might be used is much more limited than if LLBNs are intercalated between SC and FEF input and the EBNs.

The results presented here have appeared previously in abstract form (Keller and McPeck 1999).

METHODS

Two juvenile male *Macaca mulatta* monkeys were used for this study. All experimental protocols were approved by the Institutional Animal Care and Use Committee at the California Pacific Medical Center and complied with the guidelines of the Public Health Service policy on Humane Care and Use of Laboratory Animals.

Surgical preparation

Surgery was performed under isoflurane anesthesia and aseptic conditions. Heart rate, respiratory rate, body temperature, blood pressure and oxygenation were monitored for the duration of the surgery. Four devices were implanted in each monkey. 1) A stainless steel chamber was placed stereotactically on the skull, slanted posteriorly at an angle of 38° in the sagittal plane, and aligned approximately perpendicular to the surface of the SC. 2) Another stainless steel chamber was mounted stereotactically on the skull, slanted laterally in the frontal plane at an angle of 25°, and aligned on the OPN region. 3) A hollow, stainless steel pedestal was positioned vertically near the center of rotation of the head. The pedestal mated to a threaded rod mounted on the primate chair and served as a restraint device in subsequent experiments. The chambers and the pedestal were fixed to the skull with dental acrylic and small titanium bone screws. 4) A coil of Teflon-coated stainless steel wire was placed under the conjunctiva of one eye using the method developed by Fuchs and Robinson (1966) and modified by Judge et al. (1980). After surgery, the monkeys were

returned to their cage and allowed to recover from the surgery. When a proper level of recovery was reached, as determined by consultation with the attending veterinarian, daily recording sessions were begun. Antibiotics (cefazolin sodium) and analgesics (buprenorphine) were administered under the direction of the veterinarian during the post-operative period.

Behavioral conditioning

Each monkey was trained to climb out of its cage into a primate chair and sit in it during the experiment. Training and subsequent experimental sessions were conducted 4–5 times a week. The monkey was given water or juice rewards for correctly executing behavioral paradigms and was allowed to work until satiation. Daily records were kept of the animal's weight and health status. Supplemental water was given as necessary, and unlimited water was provided on days when training or experimental sessions were not performed.

Behavioral paradigms, visual displays, and data storage were under the control of a real-time program running on a laboratory PC system. The monkeys were trained to fixate a spot of light and make a saccadic eye movement to the location of the spot when it jumped to a new location. The monkeys were required to keep their eyes within 1–2° of the fixation point during a randomly selected fixation interval of 400–600 ms. A Macintosh computer, which was interfaced with the PC, generated the visual displays. Visual stimuli were presented on a 29-in. color cathode ray tube (Viewsonic GA29), in synchronization with the monitor's vertical refresh. The monitor had a spatial resolution of 800 by 600 pixels and a noninterlaced refresh rate of 75 Hz. The monitor was positioned 57 cm in front of the monkey and allowed stimuli to be presented in a field of view of approximately $\pm 25^\circ$ along the horizontal meridian and $\pm 20^\circ$ along the vertical meridian. Off-line analysis of the eye movement data were performed by algorithms using velocity and acceleration criteria to detect the beginning and end of saccades. The algorithm's identification of saccades was inspected by one of the investigators to verify its accuracy.

Experimental paradigms

Before each experimental session, both chambers were opened and cleaned under aseptic conditions. Double eccentric positioning devices were loaded in the chambers, which allowed microelectrode penetrations at any location within the 12-mm diameters of the chambers. Sharpened guide tubes with tungsten microelectrodes inside were inserted through the dura in each chamber, and independent hydraulic drive systems were used to advance the microelectrodes to the desired locations in the brain.

First a microelectrode was advanced in the chamber located over the SC until the dorsal surface of the SC was encountered. This landmark was distinguished by the presence of high-frequency discharge correlated with visual transients recorded on the electrode and played on the audio monitor as the animal made spontaneous saccadic movements about the lighted room. The electrode was advanced further into the deeper layers of the SC as the animal made saccades to images that appeared on a video monitor placed in front of it. We began to test the effect of microstimulation at depths in SC where motor or visuomotor cells were first encountered. Stimulus train parameters were set at 400 spikes/s and 40 ms in duration. Stimulus pulses were bipolar with each phase set at 0.2 ms in duration. The electrode was left in place at the point in the deeper layers of the SC where the lowest threshold for evoking saccades was encountered. The point of lowest threshold was between 1.5 and 2.0 mm from the dorsal surface of the SC. The threshold currents necessary to evoke fixed vector saccades varied from 10 to 40 μA . We first determined rough coordinates of the saccadic motor map on the SC in preliminary penetrations and then, based on this map, placed the stimulating electrode at caudal locations where the evoked saccades were large (20–40°) and nearly horizontal in direction. This placement of the

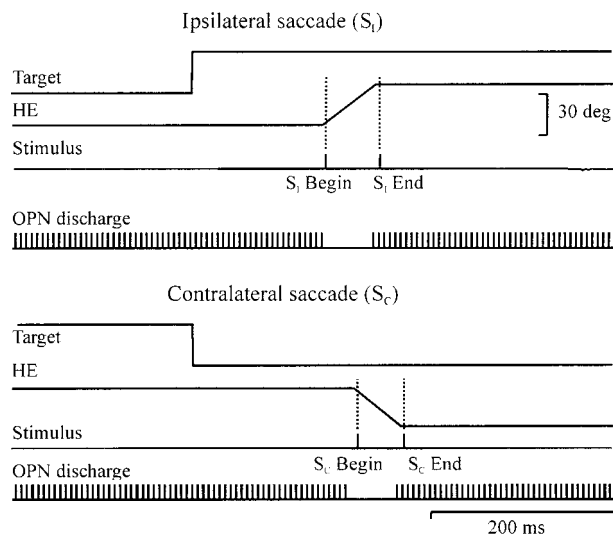


FIG. 1. Schematic layout of the times of stimulation in relationship to the underlying behavioral events during the present experiments. *Top trace* in each set of events shows the time of target jump. The *next trace* shows the horizontal eye (HE) movement produced by the horizontal target jump. The *next trace* shows the times of single-pulse stimulation of the superior colliculus (SC). Vertical dotted lines here help with visualization of the times of stimulation with respect to start and end of saccadic eye movements. The *bottom trace* shows the discharge of an omnipause neuron (OPN). S_I Begin, 4 ms after onset of ipsilateral saccades; S_I End, just after the end of ipsilateral saccades; S_C Begin, 4 ms after onset of contralateral saccades; S_C End, just after the end of contralateral saccades.

stimulating electrode was done to maximize the chance of finding direct connections to EBNs in the PPRF (Moschovakis et al. 1998). The latter authors have shown that the strength of the projections from SC to the brain stem region of the EBNs increases by more than a factor of three from rostral to caudal regions of the SC.

The SC stimulating electrode then remained in place for the rest of that day's experiment. Another electrode was advanced through a guide tube placed in the chamber located over the contralateral PPRF region of the EBNs. Burst neurons with ipsilateral, horizontal directions were isolated in this region and then were subjected to electrophysiological testing for inputs from the SC. In the remainder of this paper, we will reference saccade directions, ipsilateral or contralateral, to the side of the burst neuron being recorded. Single-pulse stimuli were delivered through the electrode in the SC while recording the extracellular potential of the burst neuron. The current of the stimulating pulses was set at $100 \mu\text{A}$ and thus was well above the level of current intensity needed in stimulus pulse trains to evoke saccades from the same SC site. At many sites we also tested with currents of $150 \mu\text{A}$. We delivered these single-pulse stimuli in pairs as the animal made ipsilateral and contralateral 30° saccades in response to target jumps on the monitor as shown on the schematic in Fig. 1. Stimulation was delivered on about one-half of the trials selected at random in a block of trials. The other trials were nonstimulated. On stimulated trials one stimulus pulse was triggered by the on-line computer program shortly after saccade onset while the other was triggered following a 10-ms delay after saccade end. Off-line analysis showed that the stimulus near saccade onset was reliably placed at 4–5 ms after saccade onset, and the stimulus near saccade end occurred at 9–16 ms after saccade end. With this schedule the SC was stimulated with the OPNs off (at the initial pulse) and with the OPNs on (at the 2nd pulse) for both ipsilateral and contralateral saccades.

Data collection and analysis

Horizontal and vertical eye position, velocity, and target position were sampled at 1 kHz and were stored on computer disk. Eye

velocity was obtained by analog differentiation of the eye position signals. The occurrence of unit discharge was determined with the use of a standard electronic window detector. The output of the window detector was stored to disk in temporal register with the analog data. Raw neural activity was also sampled at 40 kHz and stored to disk in temporal register with the eye movement data. This was done to permit off-line confirmation and correction of unit spike occurrences on the windowed data. The timing of unit events in all the off-line analyses was always determined from the onset of the stimulus pulse as determined on the 40-kHz sampled, stored records. All off-line analyses were performed in Matlab (The Mathworks).

Histology

At the completion of the recording sessions an electrolytic lesion ($20 \mu\text{A}$ for 30 s) was made in the region of PPRF where burst neurons had been recorded. After a 4-day period the animals were deeply anesthetized and perfused through the left ventricle with isotonic saline followed by 10% Formalin. Frozen $60\text{-}\mu\text{m}$ sections were cut in the plane of the electrode penetrations. Sections were stained with cresyl violet, and the site of the lesion marker was recovered by microscopic examination to confirm that the recording sites were in the PPRF.

RESULTS

We recorded from two broad classes of cells in the present study. Figure 2 illustrates the discharge characteristics of two cells whose individual behaviors are representative of these two types. The cell whose discharge is shown in the upper plot was classified as an EBN. It discharged an intense burst of spikes before all ipsilateral saccades, and the duration of these bursts mirrored the duration of the accompanying movement. The cell shown in the lower plot was classified as an LLBN. It showed a long prelude of presaccadic spikes and a burst during ipsilateral saccades. This cell discharged best for small saccades and only slightly or not at all for large ipsilateral movements. Thus it displayed a movement field organization. Some, but not all, of the LLBNs that we studied showed a movement field organization, demonstrated by a more intense discharge for either small or large saccades but not both. In addition, some LLBNs showed a clear visual response when the cell's activity was realigned on target onset.

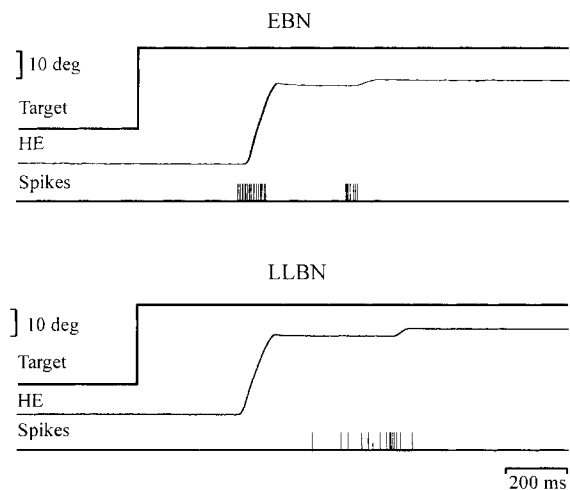


FIG. 2. Sample discharge patterns of the 2 types of burst cells recorded in the present study. Data shown for ipsilateral saccades only. EBN, excitatory burst neuron; LLBN, long-lead burst neuron.

We recorded from a total of 42 burst cells in the PPRF of 2 monkeys. We quantified the differences between EBNs and LLBNs by measuring the lead of the first spike in each cell's discharge with respect to ipsilateral saccade onset for saccades associated with the most intense burst activity. The cells that we classified as EBNs always showed a sharp onset of activity just before ipsilateral saccades, and the lead of discharge onset before the start of the movement ranged from 6 to 15 ms with a group mean of 12.5 ms. The values of the initial discharge with respect to saccade onset in cells we classified as LLBNs varied from 26 to >100 ms with a group mean of 76 ms. Based on presaccadic lead time, we classified 21 cells as EBNs and 21 as LLBNs.

We also quantified the differences between EBNs and LLBNs by counting the number of spikes in their saccade-related bursts (where the temporal limits of the bursts were defined as 15 ms before saccade onset to saccade end) for horizontal, ipsilaterally directed saccades of different sizes. We determined the regression for the number of spikes with saccade magnitude as shown for three cells in Fig. 3. The graph in Fig. 3A plots the linear regression for the EBN shown in the *top plot* of Fig. 2 and illustrates the previously reported linear relationship that exists for EBN discharge as a function of ipsilateral saccade size (see Hepp et al. 1989, for a review). The r^2 value for this cell was 0.84. In contrast, the relationship between the number of spikes in the burst and saccade size was more variable in LLBNs as illustrated by the behavior of the two cells shown in Fig. 3B. The data for the discharge shown with filled circles comes from the cell shown in the *bottom plot* in Fig. 2, which had a movement field organization. We fit the relationship of this cell's saccadic spike count as a function of saccade size with a cubic spline (solid curve) to illustrate its field preference for small saccades. Its linear regression (not shown) was negative and had an r^2 value of 0.2. The data for the discharge shown in Fig. 3B with open circles are from another LLBN. Its linear regression is shown with a dashed line, and the r^2 value of the regression for this cell was 0.58.

The r^2 values for the two classes of cells overlapped: values for EBNs ranged from 0.45 to 0.96 (group mean, 0.75), while the r^2 values for the LLBNs ranged from 0.02 to 0.74 (group mean, 0.34).

Single-pulse stimulation of the contralateral SC did not activate EBNs during either contralateral saccades or during fixation immediately after saccades. Results for a typical EBN are shown in Fig. 4. Figure 4A shows the spontaneous activity of this cell during ipsilateral saccades for four superimposed nonstimulated trials. The high-frequency discharge of this cell for large ipsilateral saccades was typical of the EBNs recorded in the present study. Figure 4, B and C, shows four superimposed stimulated trials, for the same cell, when the stimulus in the SC was delivered just after the end of ipsilateral (Fig. 4B) or contralateral (Fig. 4C) saccades. During these periods the cell was not active, OPNs were on, and the animal was actively fixating. Similar results during fixation were obtained for all 21 EBNs that we recorded. Figure 4D shows the results obtained in the same cell for four trials when the stimulus was delivered near the onset of contralateral saccades. Again the cell was not activated even though OPNs were off at this time. Similar results were obtained for all 21 EBNs. Figure 4E shows the results obtained for four trials when the stimulus was delivered near the onset of ipsilateral saccades. At this time the cell is

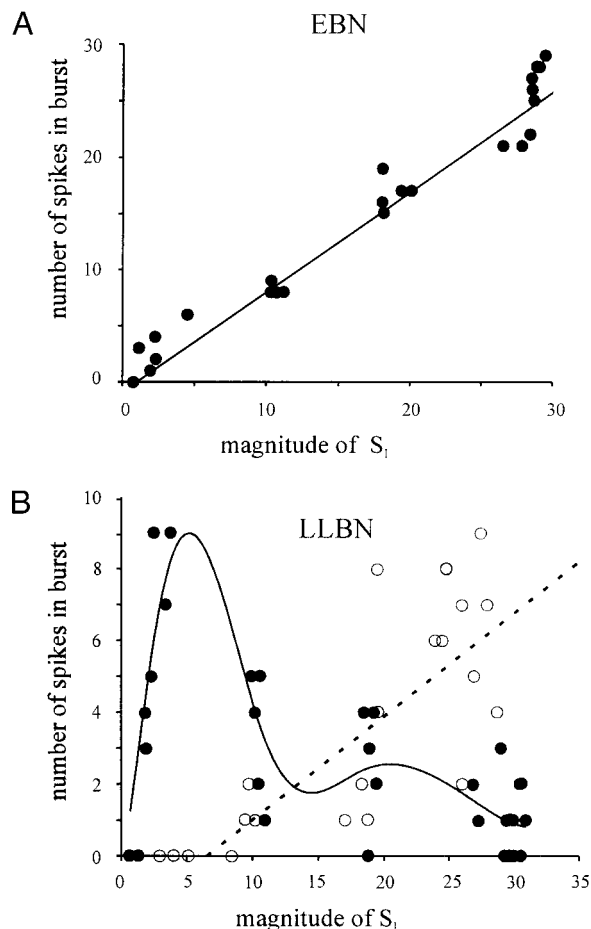


FIG. 3. The relationship between the number of spikes in the bursts and ipsilateral saccade (S_1) magnitude. A: data from 1 EBN. B: data from 2 LLBNs. One LLBN had a movement field organization (data for this cell shown with filled circles) with a preference for saccades $\sim 5^\circ$ in magnitude. The other LLBN showed an increase in the number of spikes for increasing saccade magnitude (data for this cell shown with open circles). In both A and B the straight lines are the linear regressions of the data. The data for the LLBN with a movement field were fit with a cubic spline (solid curve).

very active, but no apparent stimulus-locked activation of the cell occurs. The data in Fig. 4A were aligned on a time point 4 ms after saccade onset, which is identical to the same time of alignment used in Fig. 4E for stimulated trials. The discharge of the cell shown in Fig. 4A suggests that it might be difficult to detect a weak activation of the cell following stimulation during ipsilateral saccades due to the high spontaneous discharge rate of the cell during this time.

In an attempt to look for weak connections to EBNs from the SC, which should be exposed during ipsilateral saccades, we constructed poststimulus time histograms (PSTHs) of unit activity for stimulated and nonstimulated trials for all the EBNs and many of the LLBNs. Examples of these PSTHs for three EBNs and one LLBN are shown in Fig. 5. The data for stimulated trials were aligned on stimulus onset, and the total number of spike counts in each 0.2 ms bin was determined. Similar data for unstimulated trials were aligned on a time point 4 ms after saccade onset. Each histogram was then normalized by the total number of trials. For the histograms constructed from nonstimulated trials, the mean normalized spike count and two standard deviations from this mean were determined by computations made over the entire 12-ms inter-

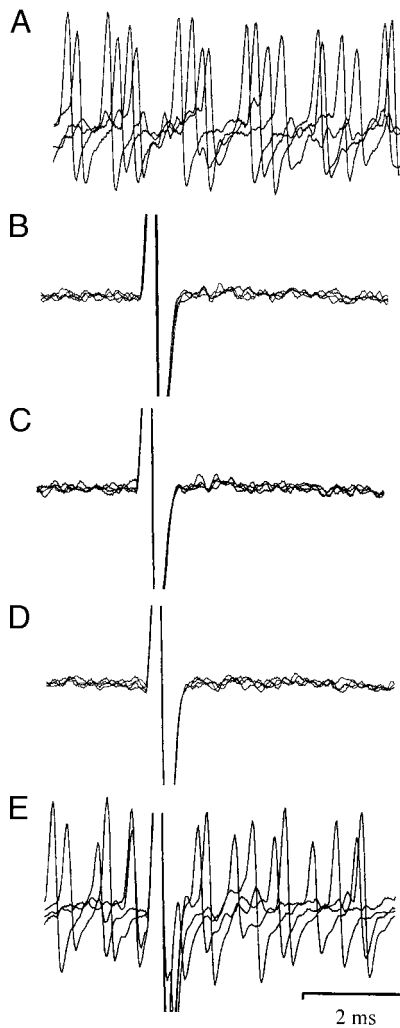


FIG. 4. Activation attempts for a typical EBN for single-pulse stimulation of the contralateral SC. For each set of traces, 4 trials are aligned on stimulation onset or, in nonstimulated trials, aligned on a similar time point with respect to the saccade (~ 4 ms after saccade onset). The large negative/positive stimulus artifact is cutoff for clarity. Negative potentials are shown as up. *A*: activity of the cell near saccade onset on nonstimulated trials. Note the high spontaneous discharge of the cell. *B*: stimulation just after the end of ipsilateral saccades. *C*: stimulation just after the end of contralateral saccades. *D*: stimulation during contralateral saccades. *E*: stimulation during ipsilateral saccades.

val of the histogram analysis. An example of the mean and the mean plus two standard deviations for one cell are shown in the *top histogram* of Fig. 5A by the solid and dashed lines, respectively. For the stimulated trials (*bottom histograms* in all sections of Fig. 5) the mean normalized spike count and two standard deviations from the mean were computed from the data in the 2-ms period of time before stimulus onset. The absence of spikes in the first two or three bins of the histograms for stimulated trials was due to the presence of a stimulus artifact in the recordings.

We determined the first time bin after stimulation onset that exceeded two standard deviations from the mean spike count and took the midpoint of this bin as the latency of the earliest activation of the cell following SC stimulation. For the cell shown in Fig. 5A the value of this latency was 1.1 ms. Various estimates ranging from 1.4 to 1.6 ms have been made for the longest latency that should be considered as monosynaptic

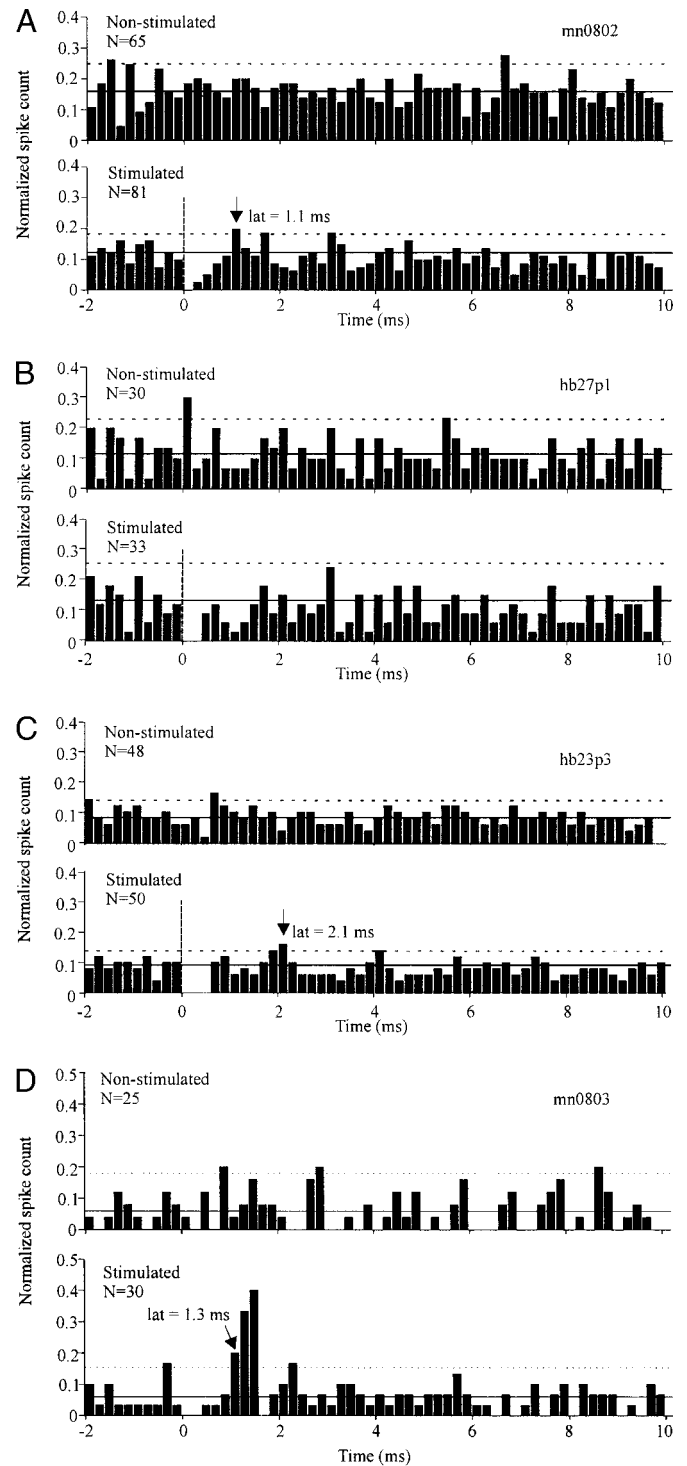


FIG. 5. Peristimulus time histograms for 3 EBNs and 1 LLBN. Each section shows data from nonstimulated trials on *top* and stimulated trials on the *bottom*. Histogram binwidth was always 0.2 ms. Since the number of trials were not the same for stimulated and nonstimulated histograms, the total bin counts were normalized by the number of trials in each. The solid horizontal line in each histogram shows the mean normalized spike count, and the horizontal dashed line shows the mean + 2 SD from the mean. These statistics were computed from the entire 12-ms record for histograms constructed from nonstimulated trials and from the 2-ms period before the onset of the stimulus for histograms constructed from trials with stimulation. Stimulation onset for the stimulated case is indicated by the dotted vertical lines. The data for the nonstimulated case were aligned on an equivalent time (~ 4 ms after saccade onset). See text for definition of latency of activation. *A–C* are for 3 EBNs and *D* is for 1 LLBN.

activation from the SC to PPRF neurons (Chimoto et al. 1996; Paré and Guitton 1994; Raybourn and Keller 1977), so that the results shown in the *bottom histogram* in Fig. 5A suggest direct connections to this cell from the SC. However, the weakness of this possible short-latency connection is highlighted by examination of the data shown in the *top histogram* in Fig. 5A, where the same cell shows occasional bins that exceed the two-standard deviation criterion even during nonstimulated trials.

The data for another cell shown in Fig. 5B were typical of the results obtained for many EBNs in our sample. The normalized spike count in stimulated trials never exceeded the two-standard deviation criterion in the 10-ms interval following stimulus onset. The results shown in Fig. 5C illustrate the data for a cell in which di-synaptic or longer latency connections were possibly demonstrated. This cell shows evidence of weak input from the SC, but with a latency of 2.1 ms.

In contrast, most LLBNs (17 of 21) were clearly activated at shorter latencies following SC stimulation during ipsilateral saccades, and one example using the PSTH method is shown in Fig. 5D. In addition to the histogram method, when the connections from SC are strong and direct to neurons with low firing rates, as in the case of LLBNs, the direct superposition of evoked spikes can be visually compelling and provides an alternative method of measuring latency. An example is shown in Fig. 6 for another LLBN. In Fig. 6A, for stimuli delivered during ipsilateral saccades, the cell's response follows stimulation at a mean latency of 1.5 ms, suggesting the presence of monosynaptic connections to this cell from the SC. In LLBNs activation was one-to-one with little temporal jitter in the time of activation. In Fig. 6B it may be seen that the cell is still activated when the stimuli are delivered after the end of ipsilateral saccades, but the latency of the average activation, as determined by the histogram method has increased by ~ 0.5 ms, and there is more temporal jitter in the response. The cell is also activated at this longer latency during contralateral saccades (Fig. 6C). These observations suggest a lower level of excitability for the cell after the end of ipsilateral and during contralateral saccades. Surprisingly, the cell was not activated by stimuli delivered during the time period just after contralateral saccades (Fig. 6D). All but 3 of the 17 LLBNs that could be activated during ipsilateral saccades could also be activated after the end of ipsilateral saccades (similar to the response shown in Fig. 6B), but at systematically longer latencies. For contralateral movements, 10 LLBNs were activated both during and after the saccade, 2 cells showed the pattern illustrated by the cell shown in Fig. 6, and 5 cells could not be activated either during or just after saccades.

The cell used to illustrate Fig. 6 was also one of the eight LLBNs we recorded that showed a movement field organization. For this particular cell, its movement field center was located at $\sim 5^\circ$ eccentric, and yet it was clearly activated by stimulation in the caudal SC. The same was true for the other LLBN we recorded that had a small ($< 10^\circ$) eccentric displacement of its movement field center.

Figure 7 is a summary diagram showing the activation latencies following SC stimulation during ipsilateral saccades for both EBNs and LLBNs. Following the most conservative estimate, we have placed a vertical dashed line at 1.6 ms to separate cells that could possibly receive monosynaptic input from the SC from those in which the connection is di- or

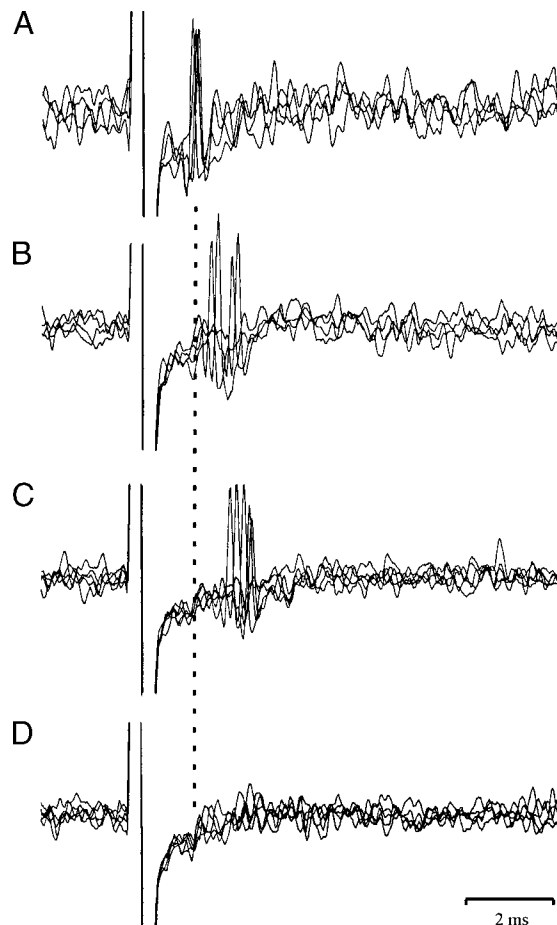


FIG. 6. Activation of an LLBN for single-pulse stimulation of the contralateral SC. For each set, 4 trials are shown aligned on stimulation onset. A: stimulation during ipsilateral saccades. B: stimulation just after the end of ipsilateral saccades. C: stimulation during contralateral saccades. D: stimulation just after contralateral saccades. The cell was not activated. The dotted vertical line shows the mean latency of activation for the stimulation set shown in A.

polysynaptic, or in which no connection at any latency could be demonstrated under the conditions of the present experiment (ND). Only one EBN of 21 tested could be activated in the monosynaptic range while 15 of 21 LLBNs fell into this class. An additional 13 EBNS were activated with latencies in the di- or polysynaptic range, and 7 could not be activated.

The determination of latencies for EBN activation following SC stimulation from standard PSTHs (e.g., the data shown in Fig. 5) may be complicated by the high spontaneous discharge of these cells during ipsilateral saccades. In trials when the EBN discharges spontaneously just after the stimulation is applied, it might be imagined that the cell would be in a refractory state when the evoked excitatory potential from the SC arrived at its membrane. It is possible that random occurrences of this type might lead to lower spike counts in the bins at latencies that would be considered in the monosynaptic range. Although we never found any evidence for this possibility in our PSTHs, we developed a new method of analysis that we believe overcomes some of the inherent difficulty in detecting the presence of the shortest latency influence of synaptic input from the SC on EBNS. In this analysis we reconstructed histograms of peristimulus spike counts during

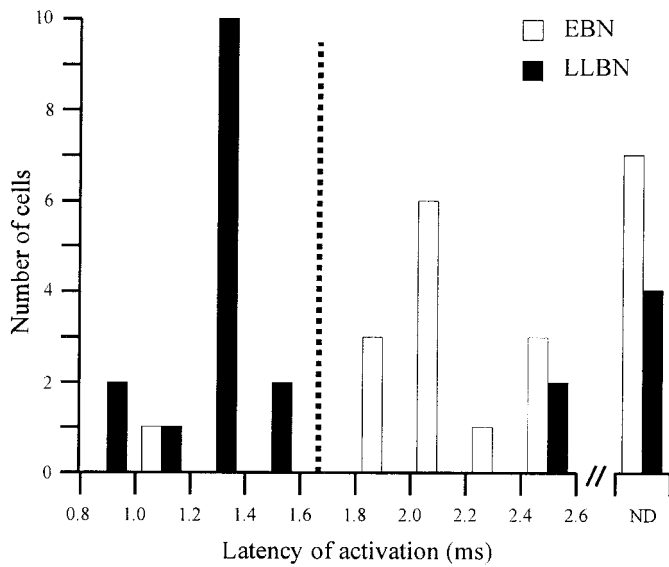


FIG. 7. Distribution of activation times for EBNs and LLBNs following SC stimulation. The dividing value for latencies with possible monosynaptic and polysynaptic connections is shown by the dashed line at 1.6 ms. ND, not driven.

ipsilateral saccades, but now aligned this data on the peak of the last spike preceding stimulus onset or the last spike preceding an equivalent time in nonstimulated trials. Figure 8 shows the combined results for 7 EBNs that had very similar discharge rates (~ 770 spikes/s) near the time of saccade onset. The arrows at *time 0* indicate the alignment point on a spike. The histogram in Fig. 8A shows the distribution of spikes for nonstimulated trials. The pacemaker-like, quasi-periodic discharge of EBNs during ipsilateral saccades when discharge is aligned on spike occurrence, which has not previously been reported, is clearly illustrated by this method of alignment. The normal-shaped distribution of spikes around the first and second peaks in Fig. 8A shows the variability expected in interspike interval around the means when no stimulations are present. No spikes are present in the bins from 0 to 0.7 ms because the cells never showed an interspike interval shorter than 0.9 ms. Figure 8B shows similar data for the same seven

cells obtained from interleaved stimulated trials and aligned on the last spike before stimulus onset. If short-latency inputs from the SC contributed directly to spike generation in EBNs following SC stimulation, the peristimulus time histogram aligned on the last spike before stimulus onset (Fig. 8B) would be expected to show a disturbance of the periodic distribution of spike occurrences seen in nonstimulated trials (Fig. 8A). The distribution of stimulus onset times after the last spike (always placed at *time 0*) is shown by the asterisks. As expected, this distribution of random stimulation times with respect to the preceding spontaneous spike is rather uniform over the interval of 0–1.3 ms. In considering the periodic spike histograms, it is important to point out that the conduction times for fibers from the SC to the region of the EBNs has been estimated to be 0.4–0.8 ms (Guitton and Munoz 1991; Raybourn and Keller 1977). If one allows 0.2 ms or less for synaptic delay (Chimoto et al. 1996), then the stimuli appearing in the first bin (centered at 0.1 ms) in the stimulus histogram in Fig. 8B should be able to phase advance the occurrence of spontaneous spikes that would have occurred by chance without stimulation in any bins from at least 1.0 ms or longer in Fig. 8A, because of the additional synaptic input provided by the synchronized monosynaptic EPSP from SC inputs, if they exist. Furthermore we know that each of these cells can discharge with an interspike interval at least as short as 1.1 ms, because they had each slowed down from the highest discharge rates they produced at burst onset. Burst onset occurred on average about 14 ms before the first interspike intervals shown in Fig. 8, because burst onset leads saccade onset by 10 ms, and the data used to fashion Fig. 8 began at 4 ms after saccade onset.

Thus on the basis of both of these arguments, the spontaneous spikes that would be expected to be most affected by stimuli occurring in the very early stimulus histogram bins (the asterisks in Fig. 8B) occur in bins at 1.3–1.9 ms. These spikes in the stimulated distribution should be advanced in time from these values expected on the basis of the nonstimulated data. In short, we should certainly be able to change, with early stimuli (optimally timed by chance), the shape of the distribution that would have been obtained without stimulation at least in the bins from 1.3–1.9 ms in

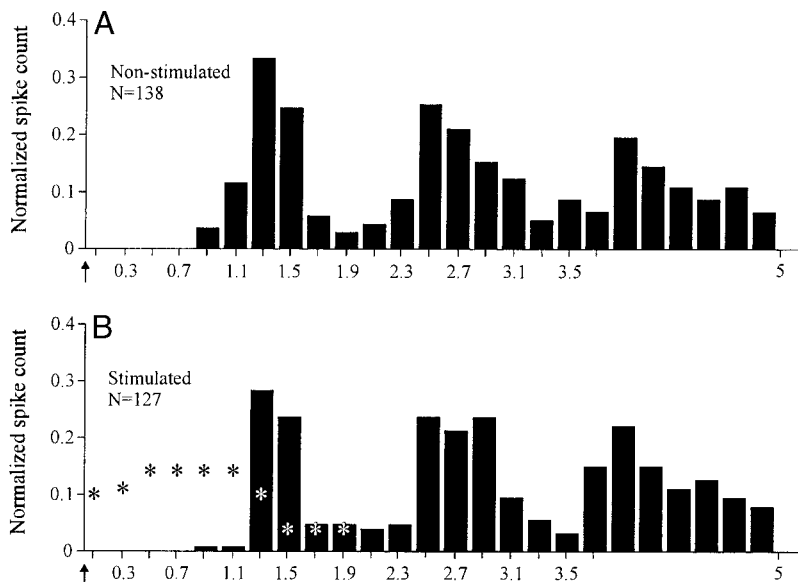


FIG. 8. Peristimulus time histograms aligned on a spontaneous spike near saccade onset. Data combined for 7 EBNs. Binwidth is always 0.2 ms. Histograms normalized by the total number of trials. A: histogram of discharge for nonstimulated trials for the 7 cells aligned on the last spike before the time point 4 ms after saccade onset (alignment point shown by the arrow). The periodic discharge of EBNs, even for data combined from several cells, is clearly shown. For clarity, the spike count in the bin at alignment point (*time 0*) is not shown. B: histogram of similar data for stimulated trials aligned on the last spike before stimulus onset. The periodic discharge of the cells is not disturbed by SC stimulation. The asterisks show the proportion of stimulus intervals after the last spontaneous spike that occurred within each 0.2-ms interval of increasing time from the last spike.

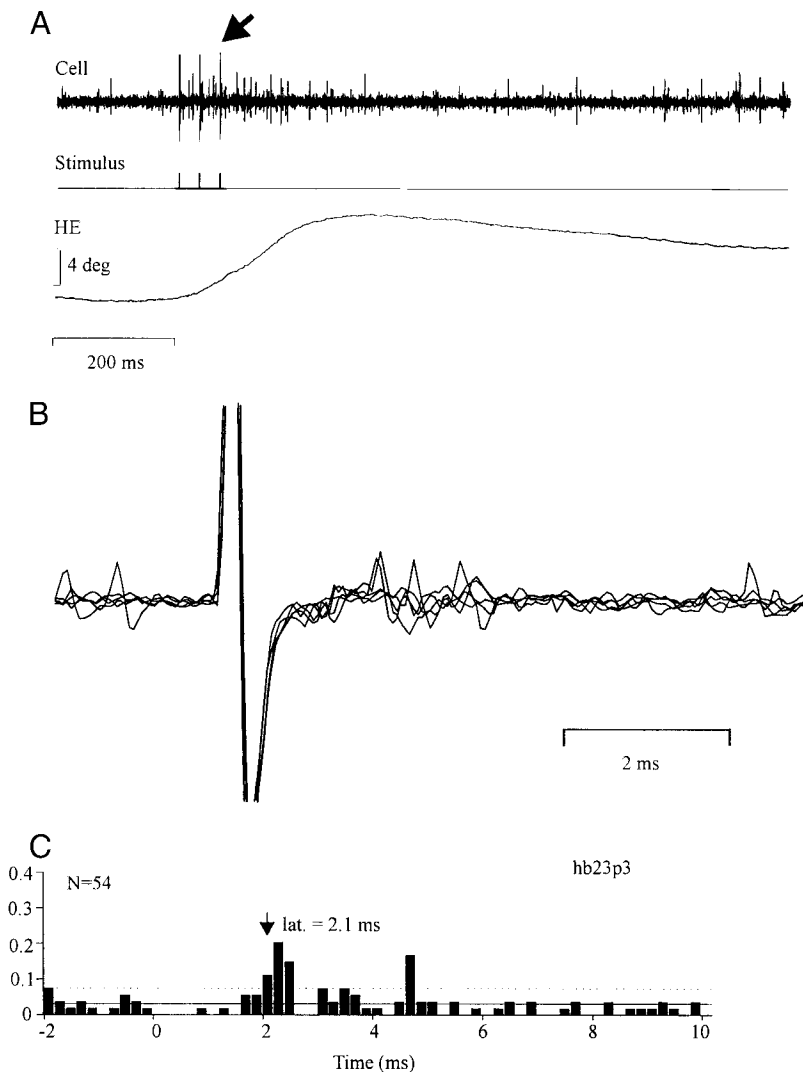


FIG. 9. Activation of an EBN during a period of drowsy ipsilateral eye movement. A: cellular activity, stimulation markers and horizontal eye movement for one episode. Oblique arrow indicates the location of the potentials from the stimulus artifact. B: high speed raw data of cell's activity during similar episodes aligned on stimulation onset. C: peristimulus time histogram for the same cell. Layout and symbols the same as in Fig. 5.

Fig. 8A. A similar argument may be applied to the distribution of spikes seen around the time of the second peak in the periodic histogram for the later occurring stimulations (stimulation histogram bins at 0.9–1.9 ms in Fig. 8B). Because of the nearly periodic firing of EBNs in the non-stimulated trials when aligned on a spontaneous spike (at least for 2 or 3 successive spikes), any changes produced by stimulation in these periodic distributions should readily be seen. Instead, statistical tests applied to the periodic distributions showed no significant change in the distributions between the data in Fig. 8B and Fig. 8A for the time intervals from 1.3 to 3.3 ms (Wilcoxon rank sum test, $P = 0.35$).

We also found further corroborating results when SC stimulations were delivered during drowsy states in the monkeys for six EBNs. In this state the animal frequently makes repetitive, back and forth drifting eye movements. When OPNs and EBNs were recorded during this state, it was found that the former cells become silent while the latter cells discharge at low sporadic rates during every ipsilateral drifting eye movement (Raybourn and Keller 1977). An example of this behavior for an EBN is shown in Fig. 9. Figure 9A shows one such episode in which the animal's eyes are initially drifting in the contralateral direction but then reverse their direction of move-

ment and begin a rapid drift in the ipsilateral direction (upward on the figure). The EBN shows a weak burst of discharge during this movement. Three-pulse stimulation in the SC (oblique arrow) with inter-pulse intervals of 33 ms was manually triggered during these episodes of rightward drift. The stimulus artifacts and the cell's discharges can be seen on the raw recording shown in the *top trace*. The cell's activity-aligned stimulation pulses, delivered during similar periods of ipsilateral eye drift and low-frequency firing, are shown in Fig. 9B (data aligned on stimulation onset). A peristimulus time histogram (Fig. 9C) was constructed for this cell, and the activation latency was determined by the same method used in Fig. 5. The latency to activation for this cell was found to be 2.1 ms, which was the same time determined by the histogram analysis used for this same cell in Fig. 6C during ipsilateral saccades. Similar results were obtained in the other five cells as shown in Table 1. In particular, in no case did we detect evidence for the presence of direct connections in any of the six cells in the drowsy state.

DISCUSSION

The results obtained in the present experiment support our previous finding that EBNs in the monkey do not generally

TABLE 1. Comparison of latencies of activation for excitatory burst neurons derived from histograms aligned on stimulation onset during ipsilateral saccades and from histograms aligned on stimulation onset during ipsilateral drifting movement during a drowsy state

	Cell					
	<i>hb22p3</i>	<i>hb23p3</i>	<i>hb24p1</i>	<i>hb26p1</i>	<i>hb26p1</i>	<i>mn0706</i>
Ipsi saccade	1.9	2.1	1.8	ND	2.5	ND
Drowsy state	2.0	2.1	2.0	5.1	2.5	ND

All values are latency of activation in ms. ND, not driven.

receive direct input from the SC (Raybourn and Keller 1977), but fall short of proving that no such connections exist, because of difficulties in interpretation when stimuli are delivered during ipsilateral saccades. Nevertheless, our results correct a technical problem present in our previous experiment in which the single-pulse stimuli in the SC were delivered with the animals fixating. Because OPNs are discharging rapidly during these intervals when the animals' eyes are stationary, and, in addition, are known to inhibit EBNs, it was possible that we failed to detect the presence of direct connections in our earlier studies due to inhibition from OPNs. Figure 10 shows a schematic model that can be used to explain the present results. The majority of LLBNs (15/21) showed short-latency activation in the monosynaptic range (<1.6 ms), while only one (of 21) EBNs was activated in this range. The mode of the distribution for activation latency in EBNs was 2.1 ms, and many EBNs had longer latencies or could not be activated at all. The additional delay in EBNs in comparison to LLBNs suggests that EBNs are activated by di- or polysynaptic pathways from the SC. A similar conclusion was reached by Miyashita and Hikosaka (1996) in stimulation studies in the monkey. They stimulated the SC during ongoing saccades and found that the earliest detectable perturbation of the eyes' trajectory occurred at 8 ms after stimulation onset. Based on estimated conduction delays and the latency present in eye movements evoked by stimulation in the region of the EBNs, they argued that the connection from SC to EBNs was at least disynaptic.

If inhibitory input from OPNs were the only input preventing EBNs from being activated during fixation, then the latter cells should be readily activated during contralateral saccades when OPNs are off. Instead, we were unable to activate any EBN during contralateral saccades. In Fig. 10 we suggest that inhibition from contralateral IBNs, which are very active during contralateral saccades, provides an additional inhibitory input that prevents the activation of EBNs during contralateral saccades. This suggestion is supported by anatomic evidence (Graybiel 1977; Strassman et al. 1986). Another opportune time to test EBNs for monosynaptic input would be during vertical saccades. In this state the OPN inhibition to EBNs would be off. The crossed inhibition from IBNs, which is probably direction specific for horizontal movements, would also be off, but the discharge of horizontal EBNs would be low or absent. Unfortunately we did not conduct tests of this type in the current series of experiments.

Although many LLBNs (10/21) could be activated during all the states tested in the present experiments (during contralateral and ipsilateral saccades and just after the end of saccades in both directions), others (7/21) showed state-dependent activation patterns or could not be activated at all (4/21). Only one LLBN showed the pattern of state-dependent activation pattern that we observed in most EBNs: activation during ipsilateral

saccades, but not during contralateral saccades or shortly after the end of either direction saccade. This pattern of activation suggests that OPNs do not play a significant role in sculpting the discharge of LLBNs. The five LLBNs that were activated by SC stimulation during ipsilateral, but not contralateral saccades could receive input from contralateral IBNs like that shown to project to EBNs in Fig. 10. This input would decrease their excitability during saccades in this direction. More complicated patterns of state-dependent activations like the LLBN shown in Fig. 6, which could not be activated shortly after the end of contralateral saccades, cannot be explained by the scheme of Fig. 10. Therefore we have left the source of

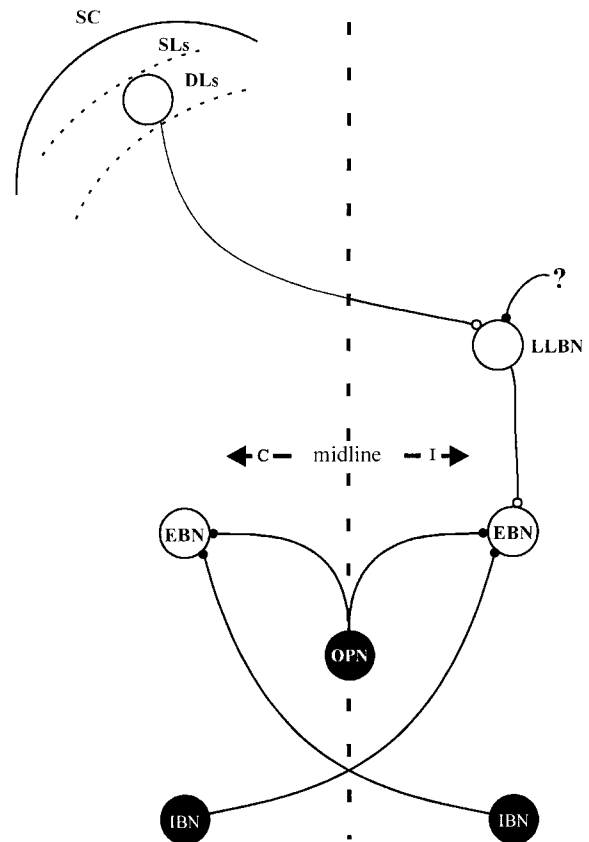


FIG. 10. Schematic summary of the connections from the SC to EBNs in the monkey. Large circles represent cells: excitatory cells shown with open and inhibitory cells with filled circles. Small open circles represent excitatory connections and small filled circles inhibitory synapses. SC, superior colliculus; SLs, superficial layers of the SC; DLs, deep layers of the SC; LLBN, long-lead burst neuron; EBN, excitatory burst neuron; OPN, omnipause neuron; IBN, inhibitory burst neuron; I, ipsilateral location to the recorded EBN; C, contralateral location to the recorded EBN. Only one-sided connections from SC to LLBN and EBN are shown, but double-sided connections of OPNs, EBNs, and IBNs are shown.

state-dependent inhibition to LLBNs in this figure with a question mark.

Grantyn and Grantyn (1976) made intracellular recordings from cat reticular neurons located close to the abducens nucleus and reported that a majority of their cells received monosynaptic input from the SC. However, in their anesthetized animals it is impossible to determine whether the cells they recorded were EBNs or LLBNs. In the present study we recorded from both types of neurons in very close proximity to each other in the PPRF. In fact, on most penetrations into this area we recorded from EBNs and LLBNs with separations of no more than 500 μm .

Chimoto et al. (1996) have conducted experiments in the alert cat similar to our present experiments in which they triggered the delivery of the SC stimulation during saccades when OPNs are known to be off. They found evidence of monosynaptic activation from the SC in 18/23 medium lead burst neurons (MLBNs) that they studied when the stimulation was delivered during ipsilateral saccades. The cells they studied were a mixture of EBNs and IBNs. Although not directly indicated in their paper, they were also unable to activate MLBNs during contralateral saccades (Y. Iwamoto, personal communication).

The reason for the marked differences in our results during ipsilateral saccades is not clear. The very high-frequency discharge of monkey EBNs during ipsilateral saccades makes it more difficult to determine whether weak direct connections exist. In the sample records from the cat that they show (Fig. 2, *D* and *G*), which are taken during nonstimulated saccades, the average firing rates of their cells are <100 spikes/s. This seems to be a very low discharge rate for EBNs. In contrast the instantaneous discharge rate for the EBNs in monkey in the present study at the time of stimulation (~ 4 ms after saccade onset) ranged from 625 to 833 spikes/s. The low discharge rate of their cells made it much easier to demonstrate the presence of connections with greater certainty. Nevertheless, we were still able to show evidence for weak connections in our peristimulus histograms made from data taken during ipsilateral saccades, but in only one case did the latency of the cell's activation following SC stimulation suggest that a monosynaptic connection exists.

We attempted to more closely match the low firing rates of their cells recorded in the cat by delivering the SC stimulation during periods of time when the monkeys were in a drowsy state. During these periods of time, EBNs were discharging at low rates as the animals' eyes drifted in the ipsilateral direction. In the six cells in which we used this procedure, none were activated in the monosynaptic range. Instead they continued to be activated at times that were similar or even later than the latencies estimated from the PSTHs constructed from data taken during ipsilateral saccades.

We believe that the most likely reason for the differences in results obtained in our study and that of Chimoto et al. (1996) is a qualitative difference in the organization of the premotor saccadic system of the monkey and cat. We speculate that this difference has developed due to the more complex behavioral repertoire of saccadic eye movements in the monkey. For example, the ability of the monkey to make antisaccades (Amador et al. 1998; Funahashi et al. 1993) has not been demonstrated in the cat. Further levels of brain stem processing

would allow more complex behavior beyond the more reflexive saccades generated by the SC.

There is also evidence in the monkey that the discharge of cells in the output layers of the SC can in some behavioral circumstances be more dissociated from the discharge of EBNs than would be expected if strong, direct connections existed from the former to the latter cells. In some cases different intensities or patterns of SC discharge can be associated with saccades that are similar in size and velocity (Edelman and Keller 1996, 1998; Everling et al. 1999). In other cases saccades of different size, speed, or direction can be produced with similar SC activity (Frens and Van Opstal 1997; Keller and Edelman 1994; Keller et al. 1996; Stanford and Sparks 1994). Explanations for these behaviors are more logically made, if at least another layer of further neural processing exists between SC output and the final premotor level of processing (the EBNs).

We thank M. Mejia for providing excellent histological support.

This work was supported by National Eye Institute Grants R01 EY-0680 to E. L. Keller and 5 F32 EY-06881 to R. M. McPeck.

REFERENCES

- AMADOR N, SCHLAG-REY M, AND SCHLAG J. Primate antisaccades. I. Behavioral characteristics. *J Neurophysiol* 80: 1775–1786, 1998.
- CHIMOTO S, IWAMOTO Y, SHIMAZU H, AND YOSHIDA K. Monosynaptic activation of medium-lead burst neurons from the superior colliculus in the alert cat. *J Neurophysiol* 75: 2658–2661, 1996.
- EDELMAN JA AND KELLER EL. Activity of visuomotor burst neurons in the superior colliculus accompanying express saccades. *J Neurophysiol* 76: 908–926, 1996.
- EDELMAN JA AND KELLER EL. Dependence on target configuration of express saccade-related activity in the primate superior colliculus. *J Neurophysiol* 80: 1407–1426, 1998.
- EVERLING S, DORRIS MC, KLEIN RM, AND MUNOZ DP. Role of primate superior colliculus in preparation and execution of anti-saccades and pro-saccades. *J Neurosci* 19: 2740–2754, 1999.
- FRENS MA AND VAN OPSTAL AJ. Monkey superior colliculus activity during short-term saccadic adaptation. *Brain Res Bull* 43: 473–483, 1997.
- FUCHS AF, KANERO CRS, AND SCUDDER CA. Brainstem control of saccadic eye movements. *Annu Rev Neurosci* 8: 307–337, 1985.
- FUCHS AF AND ROBINSON DA. A method for measuring horizontal and vertical eye movement chronically in the monkey. *J Appl Physiol* 21: 1068–1070, 1966.
- FUNAHASHI S, CHAFEE MV, AND GOLDMAN-RAKIC PS. Prefrontal neuronal activity in Rhesus monkeys performing a delayed anti-saccade task. *Nature* 365: 753–756, 1993.
- GRANTYN AA AND GRANTYN R. Synaptic actions of tectofugal pathways on abducens motoneurons in the cat. *Brain Res* 105: 269–285, 1976.
- GRAYBIEL AM. Direct and indirect precollicular pathways of the brainstem: an autoradiographic study of the pontine reticular formation in the cat. *J Comp Neurol* 175: 37–78, 1977.
- GUITTON D AND MUNOZ DP. Control of gaze shifts by the tectoreticulospinal system in the head-free cat. I. Identification, localization and effects of behavior on sensory responses. *J Neurophysiol* 66: 1605–1623, 1991.
- HARTING JK. Descending pathways from the superior colliculus: an autoradiographic analysis in the rhesus monkey (*Macaca mulatta*). *J Comp Neurol* 173: 583–612, 1977.
- HEPP K AND HENN H. Spatio-temporal recording of rapid eye movement signals in the monkey paramedian pontine reticular formation (PPRF). *Exp Brain Res* 52: 105–120, 1983.
- HEPP K, HENN V, VILIS T, AND COHEN B. Brainstem regions related to saccade generation. In: *The Neurobiology of Saccadic Eye Movements*, edited by Wurtz RH and Goldberg ME. Amsterdam: Elsevier, 1989, p. 105–212.
- JUDGE SJ, RICHMOND BJ, AND CHU FC. Implantation of magnetic search coils for measurement of eye position: an improved method. *Vision Res* 20: 535–538, 1980.
- KELLER EL. The brainstem. In: *Eye Movements*, edited by Carpenter RHS. London: Macmillan, 1991, p. 200–223.

- KELLER EL AND EDELMAN JA. Use of interrupted saccade paradigm to study spatial and temporal dynamics of saccadic burst cells in superior colliculus in monkey. *J Neurophysiol* 72: 2754–2770, 1994.
- KELLER EL, GANDHI NJ, AND WEIR PT. Discharge of superior collicular neurons during saccades made to moving targets. *J Neurophysiol* 76: 3573–3577, 1996.
- KELLER EL AND MCPEEK RM. State dependent activation of paramedian pontine reticular formation (PPRF) burst neurons by superior collicular stimulation in monkey. *Soc Neurosci Abstr* 25: 6, 1999.
- LEICHNETZ G, SMITH DJ, AND SPENCER RF. Cortical projections to the paramedian tegmental and basilar pons in the monkey. *J Comp Neurol* 228: 388–408, 1984.
- MIYASHITA N AND HIKOSAKA O. Minimal synaptic delay in the saccadic output pathway of the superior colliculus studied in awake monkey. *Exp Brain Res* 112: 187–196, 1996.
- MOSCHOVAKIS AK, KITAMA T, DALEZIOS Y, PETIT J, BRANDI AM, AND GRANTYN A. An anatomical substrate for the spatiotemporal transformation. *J Neurosci* 18: 10219–10229, 1998.
- MOSCHOVAKIS AK, SCUDDER CA, AND HIGHSTEIN SM. The microscopic anatomy and physiology of the mammalian saccadic system. *Prog Neurobiol* 50: 133–254, 1996.
- OLIVIER E, GRANTYN A, CHAT M, AND BERTHOZ A. The control of slow orienting eye movements by tectoreticulospinal neurons in the cat—behavior, discharge patterns and underlying connections. *Exp Brain Res* 93: 435–449, 1993.
- PARÉ M AND GUITTON D. The fixation area of the cat superior colliculus: effects of electrical stimulation and direct connection with brainstem omnipause neurons. *Exp Brain Res* 101: 109–122, 1994.
- RAYBOURN MS AND KELLER EL. Colliculoreticular organization in primate oculomotor system. *J Neurophysiol* 40: 861–878, 1977.
- SEGRAVES MA. Activity of monkey frontal eye field neurons projecting to oculomotor regions of the pons. *J Neurophysiol* 68: 1967–1985, 1992.
- STANFORD TR AND SPARKS DL. Systematic errors for saccades to remembered targets: evidence for a dissociation between saccade metrics and activity in the superior colliculus. *Vision Res* 34: 93–106, 1994.
- STANTON GB, GOLDBERG ME, AND BRUCE C. Frontal eye field efferents in the macaque monkey. I. Subcortical pathways and topography of striatal and thalamic terminal fields. *J Comp Neurol* 271: 473–492, 1988.
- STRASSMAN A, EVINGER C, MCCREA RA, BAKER RG, AND HIGHSTEIN SM. Anatomy and physiology of intracellularly labelled omnipause neurons in the cat and squirrel monkey. *Exp Brain Res* 67: 436–440, 1987.
- STRASSMAN A, HIGHSTEIN SM, AND MCCREA RA. Anatomy and physiology of saccadic burst neurons in the alert squirrel monkey. II. Inhibitory burst neurons. *J Comp Neurol* 249: 358–380, 1986.